Bulletin of the New Zealand Society for Earthquake Engineering, Vol. 53, No. 4, December 2020

LATERAL SHEAR STRENGTH OF RECTANGULAR RC COLUMNS SUBJECTED TO COMBINED P-V-M MONOTONIC LOADING

Aysha M. Zeneeb[1], Rupen Goswami[2] and C. V. R. Murty[3]

(Submitted *November 2019*; Reviewed *March 2020*; Accepted *July 2020*)

ABSTRACT

An analytical method is presented to estimate lateral shear strength (and identify likely mode and location of failure) in reinforced concrete (RC) cantilever columns of rectangular cross-section under combined axial force, shear force and bending moment. Change in shear capacity of concrete with flexural demand at a section is captured explicitly and the shear resistance offered by concrete estimated; this is combined with shear resistance offered by transverse and longitudinal reinforcement bars to estimate the overall shear capacity of RC columns. Shear–moment (*V-M*) interaction capacity diagram of an RC column, viewed alongside the demand diagram, identifies the lateral shear strength and failure mode. These analytical estimates compare well with test data of 107 RC columns published in literature; the test data corresponds to different axial loads, transverse reinforcement ratios, longitudinal reinforcement ratios, shear span to depth ratios, and loading conditions. Also, the analytical estimates are compared with those obtained using other analytical methods reported in literature; in all cases, the proposed method gives reasonable accuracy when estimating shear capacity of RC columns. In addition, the method provides insights into the shear resistance mechanism in RC columns under the combined action of *P-V-M*, and it is simple to use.

INTRODUCTION

RC columns and bridge piers are subjected to combined axial, shear, and bending *(P-V-M*) effects during earthquakes. Poor performance (primarily brittle shear failure of piers) of RC bridges in past earthquakes, led to analytical and experimental studies over the past several decades worldwide towards understanding behaviour of RC members under combined load effects. Analytically estimating lateral shear strength of RC members is challenging owing to nonlinear behaviour under combined *P-V-M* actions. Flexural strength is dependent primarily on the level of imposed *P* and (*V/M*). In addition, nonlinearity arises due to cracking of concrete followed by inelasticity in steel reinforcement bars in tension, and in concrete in compression. Neglecting interaction of these combined effects of *P-V-M* overestimates lateral load carrying capacity of RC members [1]. In general, shear capacity decreases with increase in flexural demand, particularly in regions of high inelasticity (*i.e.*, plastic hinge regions) [2]. Thus, a robust analytical method is required to capture realistic behaviour of RC members subjected to earthquake shaking effects.

Studies to estimate response of RC members subjected to combined load effects initiated during the late 19th century and early 20th century by Ritter (1899) and further improved by Morsch (1902) were sectional or semi-empirical methods, but gave results consistent with experimental findings. These methods use Truss Models and idealize the RC member subjected to shear and bending [3] with diagonal compression struts of concrete inclined at 45˚ to the longitudinal axis, and with the steel bars; they constitute a truss and resist the applied forces on the beam. Although these truss models overestimate the shear capacity, they are employed with some modifications owing to their simplicity and reasonable accuracy to estimate shear capacity [4-12].

The truss models estimate zero shear capacity for members without shear reinforcement, because the tensile strength of concrete is neglected. Hence, an additional term was included in design codes to account for tensile strength of concrete using an empirical expression for nominal shear strength of concrete at the diagonal cracking load, based on the then available results from experimental studies on concrete members [13, 14]. Additional research on truss models led to generalization of angle of inclination of concrete struts, and to incorporate effects of transverse and longitudinal steels [15, 16]. Three *equilibrium equations* were derived considering varying strut angle, which explained the reason for yielding of both transverse and longitudinal bars at failure. These models, known as *Equilibrium Plasticity Truss Models*, estimated the strut angles using minimum energy principles. To extend their applicability to lightly loaded members and to regions of members, which do not require shear reinforcement, these models were refined with an additional term for concrete contribution [17, 18].

To further improve the estimates from Truss Models, another model was suggested with *compatibility conditions* included to estimate the strut angles; this *Compression Field Theory* [19] assumed strut angles to coincide with the direction of principal compressive strain. After cracking of concrete, shear is assumed to be resisted by an array of diagonal compressions struts. This method evaluated biaxial stress and strain conditions in an RC member subjected to combined load effects. It neglected the tensile strength of concrete, which led to overestimation of deformation. Further verification of the theory with number of test results from RC members subjected to combined *P-V* effects led to further modification of the theory, and was called *Modified Compression Field Theory* [20]. Based on experimental data, constitutive relations were proposed of concrete in tension and of reinforced concrete in tension and compression. Effects were included in the model of local stress conditions at crack locations, strain softening and

[1] *Associate Professor, Rajagiri School of Engineering and Technology, Kochi, INDIA, aysha_z@ymail.com*
[2] *Corresponding Author, Associate Professor, Indian Institute of Technology Madras, Chennai, INDIA, rg@iitm.ac.in*
[3] *Professor, Indian Institute of Technology Madras, Chennai, INDIA, cvrm@iitm.ac.in*

tension stiffening. Around the same time, a unified *Softened Truss Model* was proposed considering *equilibrium*, *compatibility* and *softened stress strain relationships*, which helped to estimate both strength and deformation capacities of RC members subjected to shear and torsion along with post-cracking loading history [21]. The model provided results with reliable accuracy for a range of members, including deep beams, low rise structural walls, frames with structural walls, and members subjected to torsion. Subsequently, many *Truss Arch Models* were proposed to estimate shear capacity of RC members, particularly shear critical columns [2, 22-24]. In these models, the shear force acting on an RC member was considered to be transferred partly by *truss action* and partly by *arch action*, primarily depending on shear span to depth ratio. The key parameters considered in most models include axial load ratio, longitudinal and transverse reinforcement ratios and their arrangement, and shear span to depth ratio; effects of reversed cyclic loading was accounted for.

Further, several numerical and analytical methods were proposed, where *P-V-M* interaction was considered using *macro* models [25-28] and *micro* (fibre-based) beam-column elements [29, 30] with additional features to capture shear deformations and dynamic response. While some methods used *Timoshenko Beam Theory* to quantify the shear resistance mechanism (considering equilibrium between concrete and transverse steel through truss action, and then superimposing the fibre beam element), the others used semi-empirical approach to consider the *P-V-M* interaction. In the fibre beam element, a nonlinear shear force-shear deformation law was used to analyse RC members. These methods have proved to be efficient in the analysis of shear critical members. Some of these methods involve a large number of variables and require iterations to arrive at the solution, making them difficult for use in design. Some others introduce additional concepts, like incorporating static theorem of limit analysis [24]. Further, some of these methods do not provide understanding of the progressive crack behaviour of RC members under combined loading, though they provide expressions for estimating shear capacity at failure.

In this paper, a physically intuitive analytical method is proposed considering basic mechanics of the RC cross-section and member, which overcomes the said challenges in the existing methods. It estimates the lateral shear strength of RC cantilever columns with constant axial load and bending in single curvature, by integrating the well-established shear capacity estimation method with the conventional sectional analysis approach (for capturing *P-M* interaction). Also, the method captures: (a) the type of damage (whether by shear or flexure) and location of damage, and (b) effects of aspect ratio, axial load level, and amount and distribution of both longitudinal and transverse reinforcements.

Generally, monotonic backbone curves are seen to be the upper-bound envelopes of the cyclic hysteretic loops generated during cyclic loading, and in most cases, the peak load is obtained in the first significant cycle of cyclic hysteretic loops, which is as good as the monotonic test behaviour. Also, lateral deformation at peak load is not the focus of this study. Further, the cross-inclined cracking and the associated strength degradation and stiffness deterioration during hysteretic behaviour do not affect the decision making on the mode of failure, because the failure mechanism is governed by the maximum shear force demand induced in the RC column. Even though, the damage is initiated during the early loading history, the mode of failure of the RC column is determined by this maximum shear force induced in the member during the loading cycle. Furthermore, the possible transitioning from flexure failure to shear failure and vice-versa is not a concern, because the mode of failure is controlled by the relative values of global flexure and shear strengths. Therefore, monotonic loading based estimation may suffice of over-strength flexure-driven shear force demand (and shear capacity) in RC columns. Hence, this method does not use any other information of cyclic loading (except the peak load in the first significant cycle) when estimating the shear capacity of RC columns.

Accordingly, the objectives of the current study are to:

1. Develop a simple analytical method to get insight into internal resistance mechanism behavior of RC columns of rectangular cross-sections considering axial-shear-flexure interaction; and
2. Estimate the failure load, failure mode and failure location of single cantilever RC columns subjected to lateral action.

PROPOSED METHOD

The proposed method is a simple mechanistic analytical method that estimates (with reasonable accuracy) the failure (load, mode and location) of single cantilever RC columns. It involves use of expressions that have been used traditionally to analyse RC members under flexure, and hence easy to understand. Also, it focuses on the initiation of damage, whether shear or flexure; this is valuable in precluding shear failure in RC columns at the preliminary design stage. Further, it includes the effect of aspect ratio, axial load level, and amount and distribution of both longitudinal and transverse reinforcements. Compared to the existing methods, the proposed method explains in a simple way the step-wise progression of failure and the contributions of concrete and reinforcing steel to the mechanism of shear resistance.

Thus, the axial and flexural strength capacities of RC columns are determined using conventional section strength estimation approach. The lateral shear strength of RC members is determined considering contributions of: (1) concrete V_c, using *section strength approach*, and (2) transverse reinforcement (stirrups) V_{st} (through direct tensile action) and longitudinal bar V_{sl} (through dowel action), using *member strength approach*. The mechanism of resistance is established of an RC member under combined *P-V-M*, using *equilibrium of forces*, *compatibility of strains* and *uniaxial material constitutive relations* within the cross-section, and equilibrium of forces and moments within the member.

Section Behaviour

The cross-section of an RC column is discretized into a number of thin fibres of concrete (Figure 1), with width of each fibre parallel to the axis of bending; the flexural behaviour is evaluated of the cross-section through traditional moment-curvature analysis under the known axial load. The longitudinal bars are represented by equivalent fibres at the centroid of each bar. The shear capacity of each fibre of concrete is estimated corresponding to the normal stress acting on it, using the Bresler's *normal stress – shear stress failure criterion* [31]. Confinement of concrete and strain-hardening of longitudinal bars are accounted when estimating the *P-M* capacities of the section. The assumptions made are [32]:

1. Plane sections normal to the longitudinal axis of the member remain plane even after deformation;
2. Strength of concrete in tension is ignored;
3. Concrete and reinforcing bars are perfectly bonded;
4. *Normal stress f – normal strain ε* relations of concrete and steel are known and can be expressed as functions $f_c=F_c(\varepsilon_c)$ and $f_s=F_s(\varepsilon_s)$, respectively; and
5. Limiting strain in unconfined concrete is 0.004.

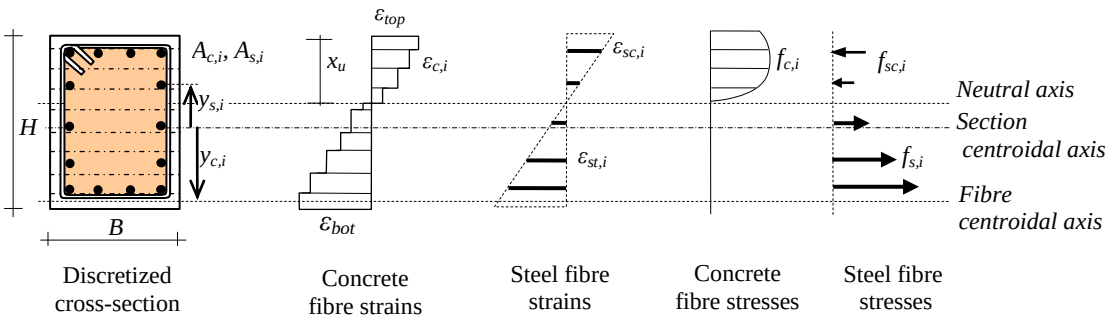

Figure 1: Discretization of cross-section and approximated normal strain and stress in fibres.

Compatibility Conditions

From the strain compatibility arising out of the linear distribution of normal strain assumed across the cross-section (Figure 1), normal strains in each concrete and steel fibre (in tension or compression) [32] are:

$$\varepsilon_{c,i} = \varepsilon_o + y_i \Delta\varphi \tag{1a}$$

$$\varepsilon_{sc,i} = \varepsilon_o + y_i \Delta\varphi \tag{1b}$$

$$\varepsilon_{st,i} = \varepsilon_o + y_i \Delta\varphi \tag{1c}$$

where,

$$\varepsilon_o = \left(\frac{\varepsilon_{top} + \varepsilon_{bot}}{2} \right) \text{ and} \tag{2}$$

$$\Delta\varphi = \left(\frac{\varepsilon_{top} - \varepsilon_{bot}}{d} \right) \tag{3}$$

in which, $\varepsilon_{c,i}$ is the average compressive strain in i^{th} fibre of concrete, $\varepsilon_{st,i}$ the average normal strain in i^{th} fibre of longitudinal steel in tension, $\varepsilon_{sc,i}$ the average normal strain in i^{th} fibre of longitudinal steel in compression, ε_0 the average normal strain in the middle fibre, ε_{top} the average strain in the top concrete fibre, ε_{bot} the average strain in the bottom concrete fibre, N the total number of fibres, d the effective depth of section, $\Delta\varphi$ the change in curvature and y_i the distance to the centroid of i^{th} fibre from the geometric centroidal axis of the cross-section.

Constitutive Relationships

The stress-strain curves of core and cover concretes differ depending on the level of confinement provided to the core by transverse reinforcement. This is determined using a standard confinement model [33] (Figure 2), where normal stress in a confined concrete fibre is given by:

$$f_{c,i} = \frac{f_{cc}^{'} x r}{r - 1 + x^r} \tag{4}$$

where,

$$x = \frac{\varepsilon_{c,i}}{\varepsilon_{cc}} \tag{5}$$

$$\varepsilon_{cc} = \varepsilon_{co}\left[1 + 5\left(\frac{f_{cc}^{'}}{f_{co}^{'}} - 1 \right) \right] \tag{6}$$

$$r = \frac{E_c}{E_c - E_{c,sec}} \text{ and} \tag{7}$$

$$f_{cc}^{'} = f_{co}^{'}\left[-1.254 + 2.254\sqrt{1 + 7.94\frac{f_l^{'}}{f_{co}^{'}}} - 2\frac{f_l^{'}}{f_{co}^{'}} \right] \tag{8}$$

in which f'_{cc} the confined compressive strength of concrete; f'_{co} is the unconfined compressive strength of concrete taken as 0.85 times the cylinder strength; f'_l the effective confining stress calculated considering rebar arrangements; f'_{ci} the normal stress in the i^{th} fibre of concrete; ε_{ci}, ε_{co} and ε_{cc} the strains corresponding to f'_{ci}, f'_{co} and f'_{cc} respectively; and E_c and $E_{c,sec}$ the initial tangent and secant moduli of concrete, respectively. The limiting strain of confined concrete is taken as [34]:

$$\varepsilon_{c,max} = 0.004 + \frac{0.6\rho_s f_{yt}\varepsilon_{su}}{f_{cc}^{'}} \tag{9}$$

where, f_{yt} and ε_{su} are the yield strength and fracture strain of transverse steel; and ρ_s the percentage of transverse reinforcement. The longitudinal and transverse steels are assumed to undergo strain hardening after yielding in the normal stress - strain curve. Further, normal stress - shear stress interaction of concrete is considered using an interaction model, originally derived based on experimental test data of a number of RC members tested under combinations of compressive and shearing stresses [31] (Figure. 2), given by:

$$\tau_{c,i} = 0.1 f_c \sqrt{0.62 + 7.86\left(\frac{f_{c,i}}{f_c} \right) - 8.46\left(\frac{f_{c,i}}{f_c} \right)^2} \tag{10}$$

where, $\tau_{c,i}$ is the average shear stress; $f_{c,i}$ the average normal stress of the i^{th} fibre of concrete; and f_c the compressive strength of concrete. In this model, a parabolic dependence is assumed of shear stress on normal stress, through a three-parameter model in terms of octahedral stresses. These three parameters are established by curve fitting of available experimental test data of number of RC members tested to failure under different combinations of compressive and shearing stresses. Other refined models available in literature [34, 35], which use four parameters (as in William Warnke Model) and five parameters (as in Ottosen Criterion, Reimann Criterion and Hsieh-Ting-Chen Criterion) as variables, provide a closer estimate of experimental test data, reflecting all characteristics, but are complex and requires more computational effort.

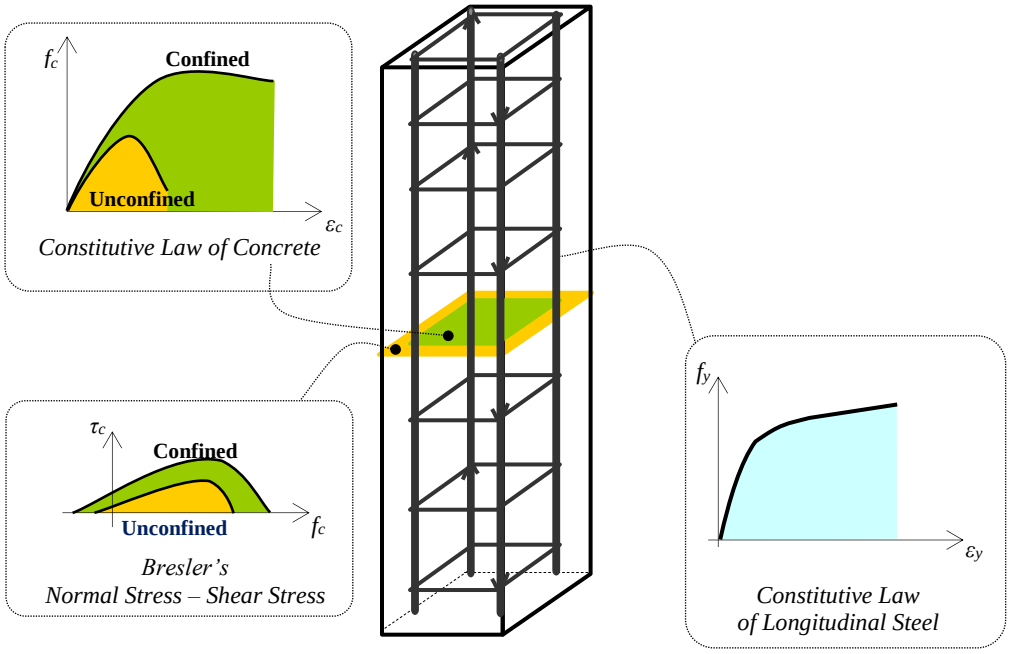

Figure 2: Schematic showing constitutive relationships considered in the proposed analytical method.

Stress-strain curve of reinforcing steel as per Indian standard specifications, IS 456 [32] is adopted in the study which is considered to be satisfactory. As per IS 456, stress remains proportional to strain up to 80% of the yield stress, f_y beyond which it is nonlinear and reaches the yield stress at strain of $(0.002+ f_y/E_s)$, where, E_s is the elastic modulus of steel. Beyond this point stress remains constant with further increase in strain. But, the curve is modified by incorporating effect of strain hardening, for a reasonable estimation of strength and ductility capacity. A bi-linear stress strain curve meeting smoothly at transition, with 15% strain hardening is considered. Strain hardening is assumed to start soon after its yielding, up to a maximum elongation of 20%.

Equilibrium Equations

A strain-based moment-curvature (M-φ) relation is derived of an RC section for applied P; the strain at the extreme top concrete fibre ε_{top} is incremented from the strain corresponding to zero curvature at that level of P, while the strain at extreme bottom fibre ε_{bot} is gradually reduced. For each distribution of normal strain across the cross-section, normal strain in concrete and steel fibres are computed using Eq. (1), and the corresponding normal stresses are computed using Eqns. (4) and (8). Then, axial force equilibrium of the section is ensured using:

$$\sum_{n=1}^{N} f_{c,i} A_{c,i} + \sum_{n=1}^{N} f_{s,i} A_{s,i} - P_{ext} = 0 \tag{11}$$

and bending moment capacity of the section is estimated (about the geometric centroidal axis of the section) for the imposed normal strain distribution as:

$$M = \sum_{n=1}^{N} f_{c,i} A_{c,i} y_{c,i} + \sum_{n=1}^{N} f_{s,i} A_{s,i} y_{s,i} \tag{12}$$

Then, for every combination of P and M, the shear strength $\tau_{c,i}$ of the i^{th} fibre is estimated using $f_{c,i}$ and Eq.(10). Then, the shear capacity contributed by concrete is computed as:

$$V_c = \sum_{n=1}^{N} \tau_{c,i} A_{c,i} \tag{13}$$

Typical normalised *shear strength – axial load* and *shear strength – bending moment* interaction curves are developed for prismatic square RC cross-sections at various axial load levels (Figure 3). The cross section geometry and reinforcement details of the prismatic RC section considered in the study are shown in Figure 3a. Grade of concrete used is assumed to have a 28-day characteristic cube compressive strength of 30 MPa, and both transverse and longitudinal reinforcement have yield strength of 415 MPa. The key observations are: (a) for any given level of axial load ratio, shear strength V_c (at M = 0) increases with increase in compressive axial load up to half the axial load capacity, and decreases rapidly with further increase in axial load ratio (Figure 3b), and (b) for any given level of axial load ratio, shear strength V_c contributed by concrete decreases with increase in bending moment demand on the section (Figure 3c); the reduction is fast as the section approaches its bending moment capacity. This observation reinforces the concept that shear capacity RC sections is significantly reduced due to flexural demand, as in potential plastic hinge regions, and thus, seismic design of such regions require consideration of P-V_c-M interaction.

Member Behaviour

Contributions to shear strength capacity of RC members are estimated as offered by concrete V_c, by transverse reinforcement (stirrups) V_{st} intercepting cracks through direct tensile action, and by longitudinal bars V_{sl} through dowel action. The total contribution of stirrups towards shear strength capacity is governed by the crack angle. The dowel action of longitudinal bar is considered when both concrete and transverse reinforcement capacities are exhausted, *i.e.*, only when the shear crack passes through the entire member depth. Crack angle and shear strength contributions of transverse and longitudinal bars are computed using simple expressions.

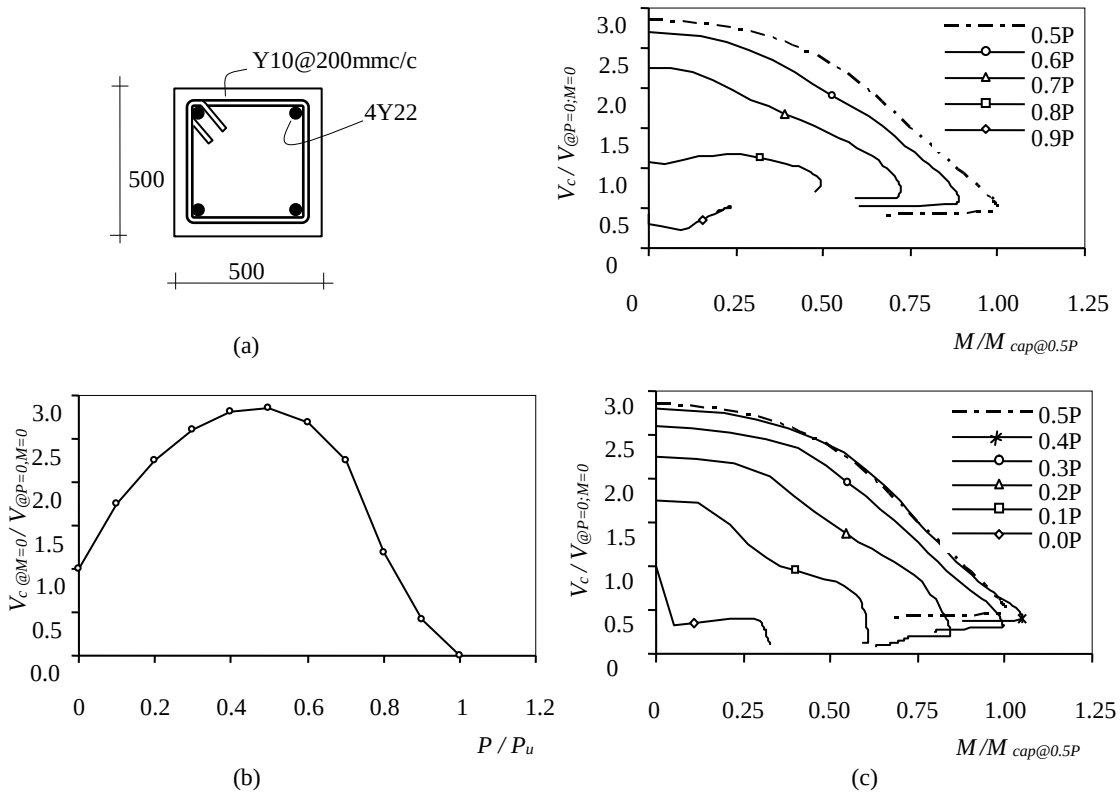

Figure 3: Shear strength of concrete for a typical rectangular RC section at different levels of axial load: (a) cross section details normalised, (b) normalised variation of shear strength capacity of concrete at zero bending moment and (c) V_c-M interaction curves.

Crack Angle

Ideal values of crack angle α in RC cantilever members in single curvature of depth H subjected to constant axial compressive force P, lateral shear force V, and bending moment M acting individually are 90˚, 45˚ and 0˚, respectively, where α is measured with respect to the direction normal to the longitudinal axis of the member. Hence, under combined action of P, V and M, the crack angle α is estimated by:

$$\alpha = \frac{\pi}{4} + \frac{1}{2}tan^{-1}\left(\frac{P}{V}\right) - \frac{1}{2}tan^{-1}\left(\frac{M}{VH}\right) \quad (14a)$$

or after eliminating V (=M/L) from Eq. (14a),

$$\alpha = \frac{\pi}{4} + \frac{1}{2}tan^{-1}\left(\frac{PL}{M}\right) - \frac{1}{2}tan^{-1}\left(\frac{L}{H}\right) \quad (14b)$$

Thus, when V is high (which is expected during strong earthquake shaking), α estimated is close to 45° in squat members with small L/H ratio, and lesser than 45° in slender members with large L/H ratio. Similarly, when V is small (expected during low level earthquake shaking), α estimated is close to 90° in squat members and close to 0° in slender members. Thus, the possible range of crack angle is $0°<\alpha<90°$. Depending on the crack angle α, a finite number of transverse reinforcement bars contribute to shear capacity of the member. The total shear strength contribution of transverse reinforcement is given by:

$$V_{st} = \sum_{i=1}^{N} F_{yi} A_{sti}\,, \quad (15)$$

where, f_{yi} is the yield strength of reinforcing bar i, A_{sti} the cross-sectional area of bar i and N the number of stirrups intercepting the crack along the length of the member.

Dowel Action

Contribution of longitudinal bars is considered through dowel action. Transfer of dowel force through shear in longitudinal bars is unlikely because of the need for large deterioration of concrete in the vicinity of the bar. Similarly, effect of kinking of the bars is insignificant as the crack width of concrete remains small relative to the bar diameter at the initiation of damage of the member. Thus, the dowel force is estimated considering plastic hinges to develop in the bars bending between two adjacent stirrups. To obtain upper bound estimate of dowel action, the bars are assumed to have full rotational fixity at the stirrups. Thus, the shear resistance offered by dowel action of n_l number of longitudinal bars V_{sl} [11] is estimated as:

$$V_{sl} = \frac{n_l d^3}{3 s_v} F_y\,, \quad (16)$$

where, s_v is the spacing of stirrups, d the diameter, F_y the yield strength, and n_l the total number of longitudinal bars contributing to dowel action.

Limiting Lateral Shear Strength of RC Members

Limiting lateral shear strength of an RC member is estimated using V-M interaction strength envelop of the cross-section as offered by un-cracked concrete for a known P, and contributions of transverse and longitudinal bars (Figure 4); nominal shear resistance offered by aggregate interlock is implicitly accounted through τ_c but not explicitly considered [10,13,31]. Figure 4 depicts how a prismatic cantilever RC member fails in shear, with uniform distribution of both transverse and longitudinal bars along the length of the member. Salient features of the interaction diagram and the shear transfer mechanism in the member are discussed below.

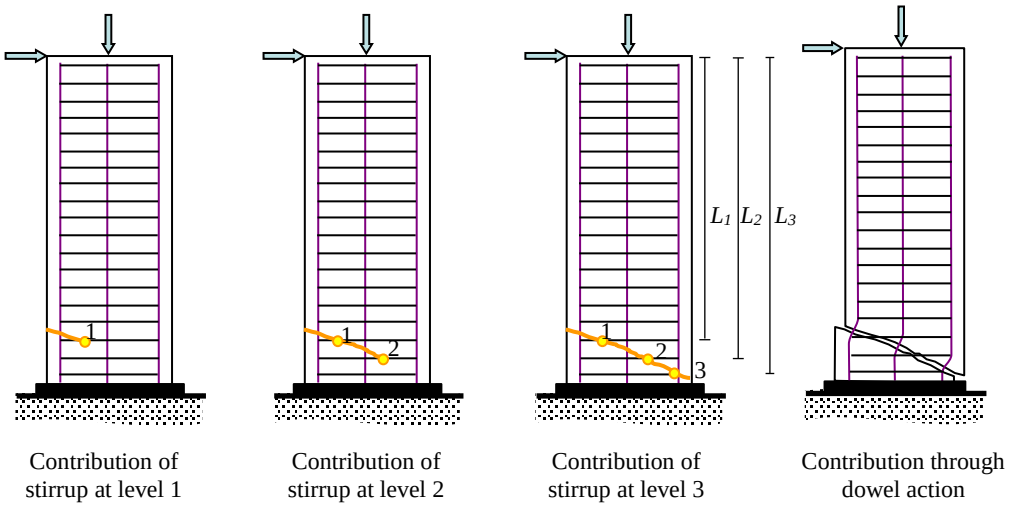

(a)

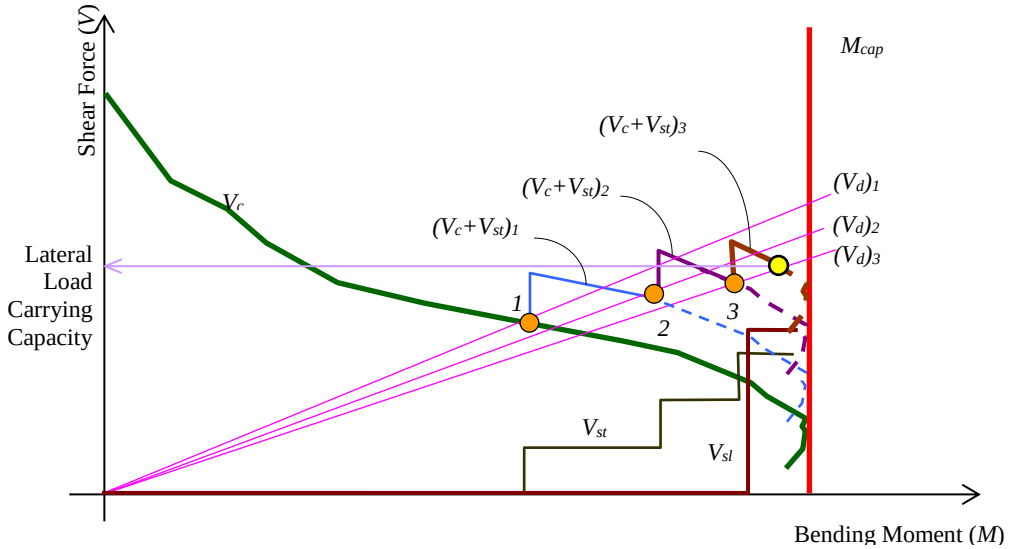

(b)

Figure 4: (a) Crack propagation across RC column (b) shear resistance mechanism in an RC member, for a considered value of compressive axial load.

(a) Salient Features - The salient features of the member *V-M* interaction diagram (Figure 4b) are:

Curve V_c represents variation of shear capacity of concrete with increase in bending moment, at a given compressive axial load, and describes the concrete shear capacity envelope;

Line V_{st} represents contribution of stirrups to lateral load carrying capacity of the member through direct tensile action;

Line V_{sl} represents contribution of longitudinal bars to the lateral load carrying capacity of the member through dowel action;

Line M_{cap} represents flexural capacity limit of the member, at stirrup levels 1, 2, and 3 (the limit is same when member is prismatic and has uniform reinforcement);

Lines V_{d1} to V_{d3} represent lateral shear force *demand* at stirrups 1, 2, and 3, respectively, corresponding to bending moments induced at stirrup levels; and

Curves $(V_c+V_{st})_{1 \text{ to } 3}$ represent shear resistance *capacity* of the member, namely the net contribution of concrete and stirrups towards the lateral load carrying capacity of the member.

(b) Shear Resistance Mechanism - The shear strength capacity of concrete reduces with increase in flexural demand as depicted by *Curve* V_c (Figure 4b). Initially, concrete alone contributes to shear resistance. As lateral load increases on the member, both *V* and *M* increase linearly, as represented by the demand *Line* $(V_d)_1$. When the demand line crosses the original concrete capacity curve (at point 1 in Figure 4b), crack (defined by angle α as in Eq.(14)) grows from the left side of the member (Figure 4a) until intercepted by the stirrup at level 1 (at a distance L_1 from the loading point at top). Then, the stirrup contributes to shear resistance, as shown by the first jump in the *Line* V_{st}. Thus, now concrete and stirrup at level 1 together contribute to capacity, as shown by *Curve* $(V_c+V_{st})_1$. With further increase in *V*, contribution of concrete V_c continues to decrease with increase in *M*. This is represented by drop in capacity *Curve* $(V_c+V_{st})_1$, until the demand *Line* $(V_d)_2$, at stirrup level 2 crosses the capacity *Curve* $(V_c+V_{st})_1$. At this stage, the shear crack grows further until intercepted by the stirrup at level 2. Again, the stirrup at level 2 (at a distance L_2 from the loading point at top) contributes to shear resistance, as shown by the

second jump in the *Line* V_{st}. Thus, now, the concrete and the stirrups at levels 1 and 2 together contribute to capacity, as shown by *Curve* $(V_c+V_{st})_2$. This process continues as the crack propagates across the cross-section; in the process, N_s number of stirrups contributes to meet the demand and is represented by the step-by-step increment in shear capacity contribution of stirrups. Once the crack passes through the cross-section (point 3 in Figure 4b), the total contribution of concrete and stirrups gets exhausted and the member fails in shear, unless the dowel action contribution as represented by the demand *Line* (V_{sl}) (which primarily contributes to the residual lateral load carrying capacity of the member), is able to resist the corresponding demand.

Failure is defined as the strength at which demand exceeds capacity. Bending moment demand varies along the height of the member. Hence, the shear capacity at each section along the height also varies. For a cantilever column, as the shear force is nearly constant throughout its height, critical section is always at the base, because shear capacity is least as the bending demand is the largest at the base. But, for a flared member or a prismatic member with varying transverse reinforcement along its height, failure may be initiated by shear at a section other than the base, as the concrete shear capacity of cross-section varies along its height (Figure 5). Thus, shear failure is likely to occur in *flared down* member at the junction between flared and prismatic sections (Figure 5a), while flexural failure is likely in *flared up* member at the base (Figure 5b).

(c) Load and Mode of Failure – The shear capacity *Curve* $(V_c+V_{st})_n$, (N_s=3 in Figure 4) together with demand *Line* $(V_d)_n$ and moment capacity *Line* M_{cap}, facilitates estimation of failure mode of a member with given cross-section. A member will fail in shear, if the demand *Line* $(V_d)_n$ crosses the supply *Curve* $(V_c+V_{st})_n$ at a lateral load level lower than the lateral load corresponding to intersection of the demand *Line* $(V_d)_n$ and the flexural capacity *Line* M_{cap} (Figure 6a). The lateral load corresponding to intersection of $(V_d)_n$ and *Curve* $(V_c+V_{st})_n$ represents the load at shear failure (as in Figure 6a with failure load of 430 kN). On the other hand, a member will fail in flexure, if the demand *Line* $(V_d)_n$ crosses the moment capacity *Line* M_{cap} at a lateral load lower than that corresponding to the intersection of demand *Line* $(V_d)_n$ and the supply: (a) *Curve* $(V_c+V_{st})_n$ (Figure 6b), or (b) *Curve* V_c alone (Figure 6c). The lateral load corresponding to intersection of $(V_d)_n$ and *Line* M_{cap} represents the lower bound lateral shear strength as the failure initiates in flexural mode (as in Figure 6c with failure load of 159 kN). As a special case, if the load corresponding to intersections of $(V_d)_n$ and M_{cap}, and that corresponding to intersection of $(V_d)_n$ and $(V_c+V_{st})_n$ are almost equal, the member is likely to fail in a mixed flexural-shear mode (as in Figure 6b with failure load of 320 kN). Thus, the lateral load capacities of the RC columns shown in Figures 6a, 6b and 6c are 430 kN, 320 kN and 159 kN, respectively.

VERIFICATION OF THE PROPOSED METHOD

The accuracy of the proposed method is examined by comparing lateral load carrying capacity and mode of failure, with those from experimental results of 107 RC specimens reported in literature [36-54]. Also, the estimated lateral load capacities of the 107 specimens are compared with those obtained using four other methods reported in literature [2, 22-24]. The distinguishing parameters in the 107 specimens are: (a) shear span-to-depth ratio of 1.0-6.6, (b) transverse reinforcement ratio 0.0014-0.0240, (c) longitudinal reinforcement ratio of 0.010-0.033, (d) axial load ratio of 0.05-0.68, (e) concrete (cylinder) strength of 20.2-49.3 MPa, (f) yield strength of reinforcement of 255-580 MPa, and (g) type of loading being double bending (*DC*) [40, 49], double ended (*2C*)

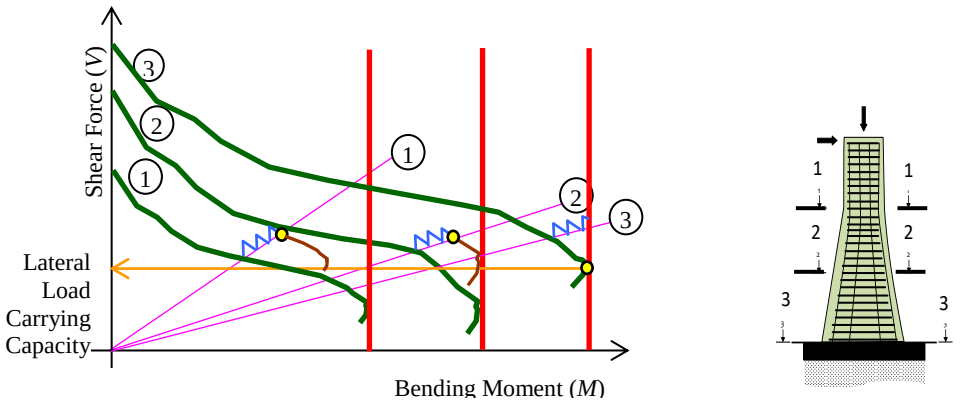

(a)

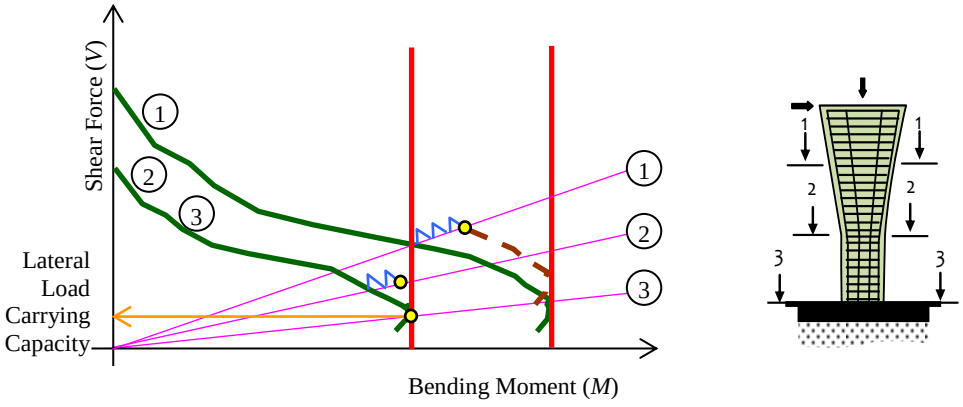

(b)

Figure 5: Typical location and modes of failure of non-prismatic RC piers (a) flared down; and (b) flared up.

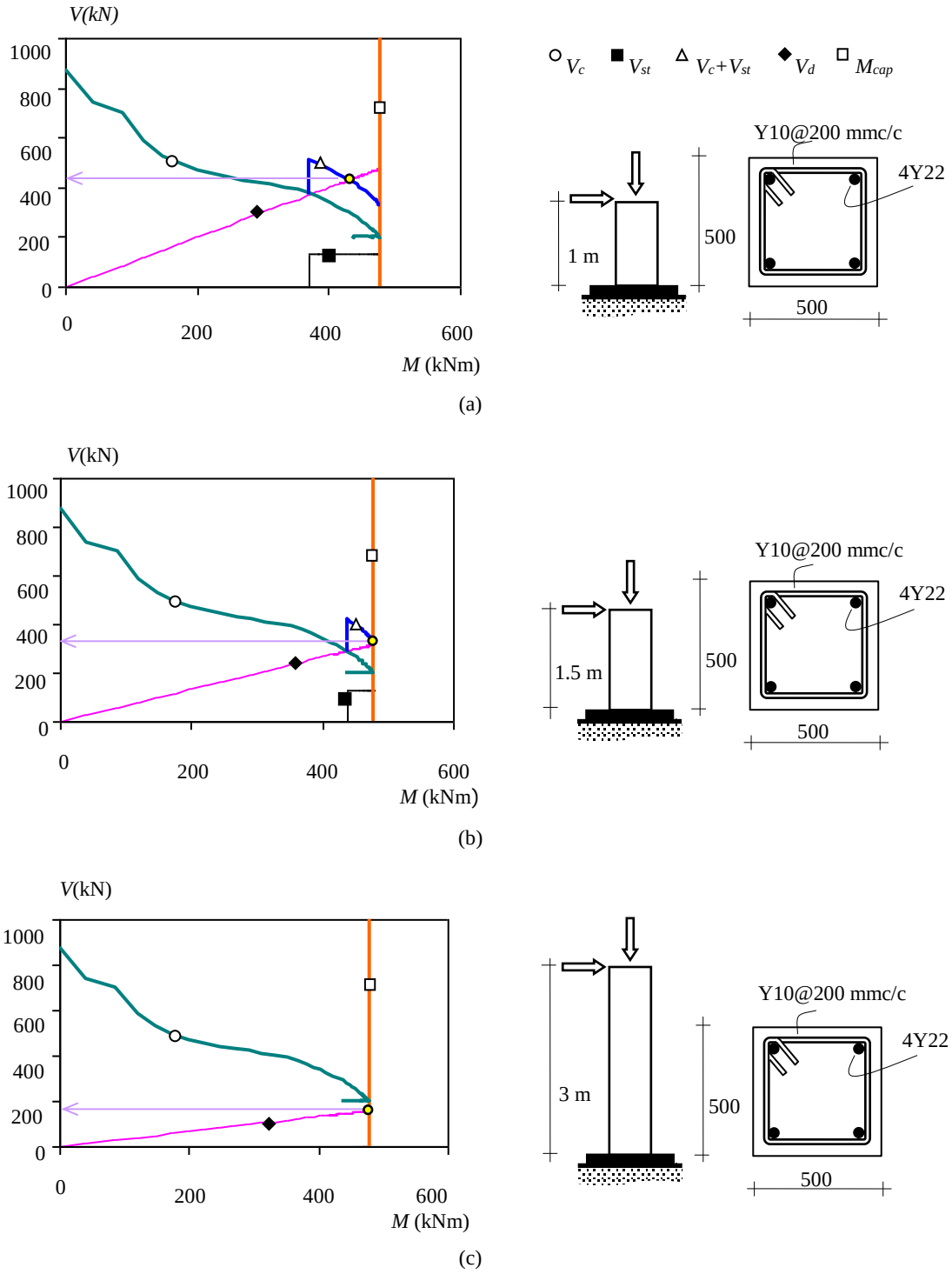

Figure 6: Typical modes of failure based on demand-capacity interaction; (a) shear failure, (b) flexural shear failure, and (c) flexural failure.

[36, 49], and cantilever columns (*C*) [45, 49]. Table 1 compares the experimental results with the values obtained using various theoretical methods. The geometrical and mechanical properties of the 107 specimens along with the estimated shear capacity and experimental results are given in Table 2, along with the estimated and observed modes of failure of the specimens.

The proposed method captures the mode of failure, in 105 of 107 cases, observed in experimental investigations. The proposed method underestimates (by about 10%) the shear strength of RC columns, particularly of specimens whose behaviour is governed by shear. Thus, the comparison of failure load estimated using proposed method V_{prop} and the experimental results V_{exp} (Figure 7a) suggests that the proposed method is consistent for both flexure and shear critical specimens; the variation of ratio of V_{prop}/V_{exp} as a function of shear span-to-depth ratio is shown in Figure 7c. Also, the estimated crack angles of the specimens correlate well with the experimentally measured crack angles (Figure 7b).

The mean ratio (of 0.91) of theoretical to experimental shear strengths of all 107 specimens considered in the study obtained using the method proposed compares well with those obtained using other theoretical methods (Table 1), although the Method 1 [2] provides the highest mean ratio of 0.95. This higher mean ratio in Method 1 is attributed to over-estimation of shear strength capacity (with mean ratio of 1.03 and standard

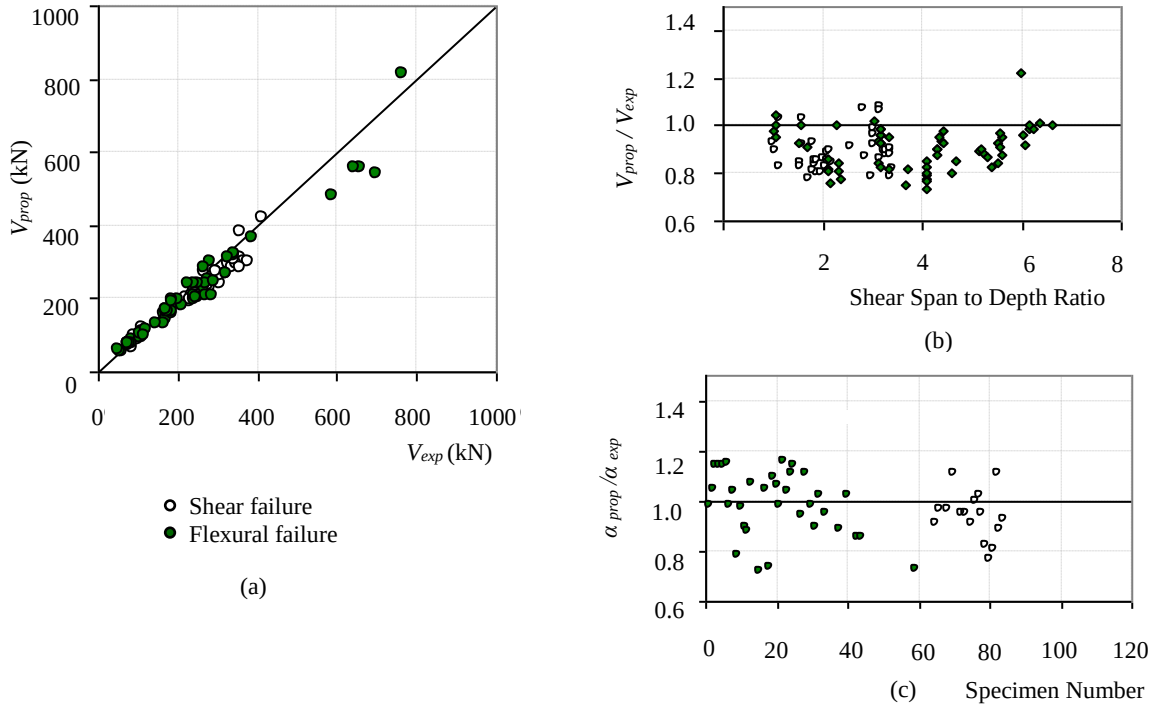

Figure 7: (a) Comparison of numerical estimates of lateral load (shear) capacity of 107 specimens to experimental values, (b) ratio of proposed to experimental shear capacity across various shear span to depth ratio, and (c) comparison of ratio of theoretical to experimental crack angle.

deviation of 0.128) of 43 shear critical specimens; this arises because the transverse steel contribution to shear strength is estimated using 30° crack angle.

This was modified in Method 2 [22], where both concrete and transverse reinforcement contributions to shear are assumed to depend on member displacement ductility. The Method 2 estimates the shear strength better with a smaller standard deviation of 0.067 for shear-critical specimens, but the percentage difference in the estimation of strength of all specimens is slightly more (about 10%) than by the other methods. Method 3 [23] also estimates shear strength of shear critical specimens with reasonable accuracy with mean ratio of 0.92, but the standard deviation is higher (0.081). This is likely to be due to the simplification made in estimating concrete and stirrup contributions to shear strength. Here, although shear strength estimation is based on the *Modified Compression Field Theory*, simplified parameters were used to estimate the crack angle and concrete contribution. Finally, the estimation of shear capacity by Method 4 [24] is consistent for both shear and flexure critical specimens, with the least error (of 8%). But, the method of computation does not provide additional insights into shear resistance mechanism in RC members.

In contrast, the Proposed Method successfully employs the conventional cross-section analysis approach and two established constitutive relations to estimate the shear strength of RC members, although the estimation is slightly conservative with a mean ratio of 0.90 and standard deviation of 0.084. The underestimation of shear capacity is possibly due to the simple assumptions made including the linear strain distribution across the cross-section and stress-strain curve of transverse steel; it is acceptable if shear strength is not overestimated, especially in safety assessment of existing RC members for possible retrofit. Finally, the error of about 10% in estimates obtained using the proposed method is comparable to those obtained using the other methods.

The advantage of the proposed method is that it provides additional insights into the mechanism of shear resistance in RC members (Figure 4). But, the sizes of the test specimens (whose results are taken from literature) are small. When this method is applied to large RC sections, like those of the bridge piers, the effect of cross-sectional size needs to be incorporated in the estimation of shear capacity; for this purpose, the size effect factors proposed in literature [55-56] may be used.

Table 1: Statistical variation of theoretical results obtained from the proposed and other methods.

Parameter	V_{theo}/V_{exp}				
	Method 1 [2]	Method 2 [22]	Method 3 [23]	Method 4 [24]	Proposed
ALL (107) SPECIMENS					
Mean	0.950	0.900	0.900	0.920	0.910
Standard Deviation	0.116	0.070	0.077	0.082	0.087
Maximum	1.390	1.160	1.160	1.160	1.220
Minimum	0.760	0.760	0.760	0.760	0.730
SHEAR CRITICAL (43) SPECIMENS					
Mean	1.030	0.920	0.920	0.910	0.890
Standard Deviation	0.128	0.067	0.081	0.074	0.078
Maximum	1.39	1.080	1.090	1.120	1.080
Minimum	0.760	0.760	0.760	0.760	0.780
FLEXURE CRITICAL (64) SPECIMENS					
Mean	0.900	0.900	0.890	0.920	0.930
Standard Deviation	0.073	0.072	0.073	0.087	0.089
Maximum	1.160	1.160	1.160	1.160	1.220
Minimum	0.760	0.760	0.760	0.770	0.730

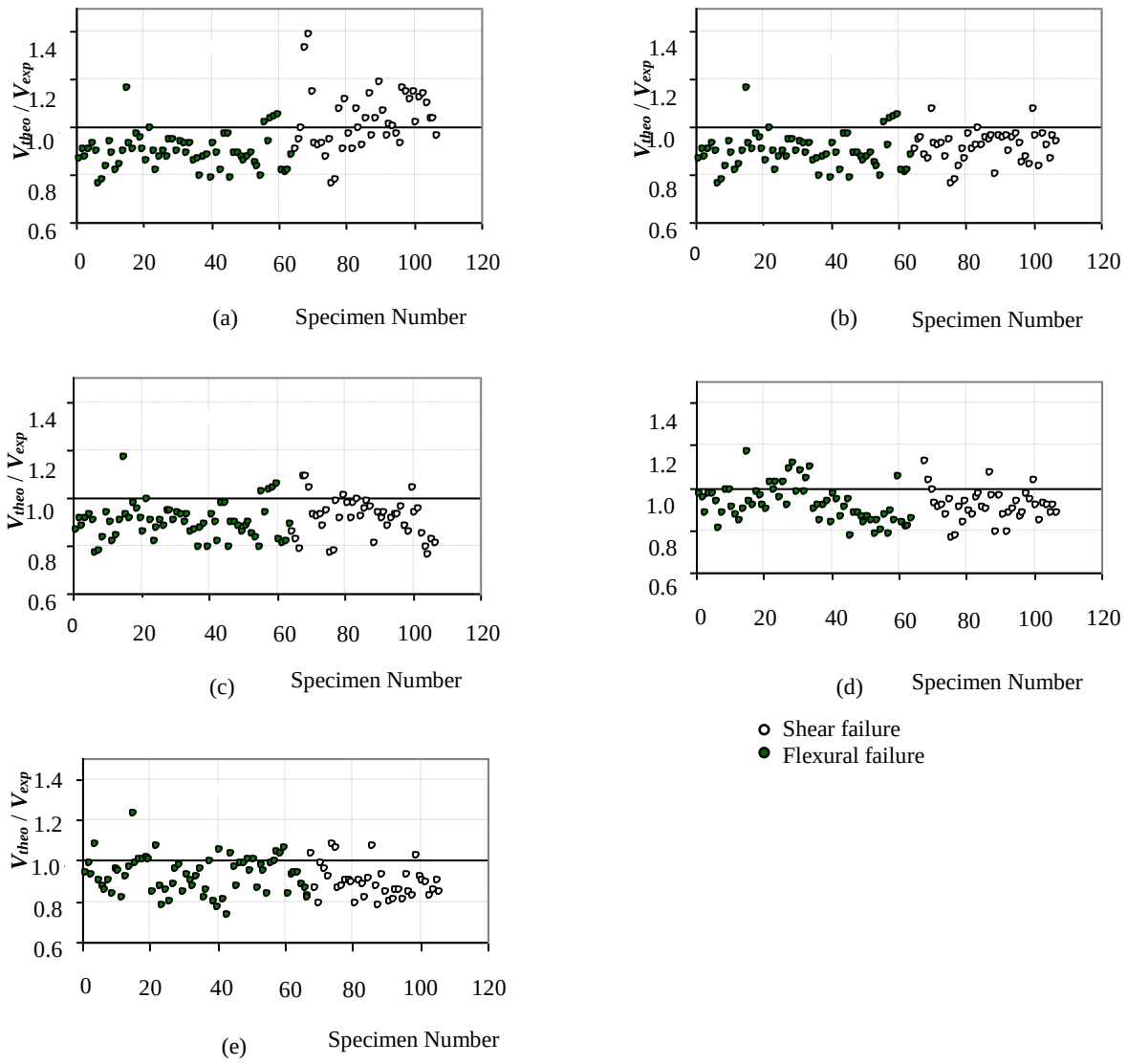

Figure 8: Comparison of ratio of theoretical to experimental shear capacity of 107 RC specimens; (a) Method 1, (b) Method 2, (c) Method 3, (d) Method 4, and (e) Proposed Method.

New Zealand Guidelines

The NZ Guidelines is generally based on Method 2 or the model proposed by Sezen and Moehle (2004) [57], which provides estimate of lateral strength alone, as:

$$V_n = V_c + V_{st} \tag{17}$$

$$V_c = k\left(\frac{0.5\sqrt{f_c'}}{a/d}\sqrt{1+\frac{P}{0.5\sqrt{f_c'}A_g}}\right)0.8A_g \tag{18}$$

$$V_{st} = k\left(\frac{A_v f_y d}{s}\right) \tag{19}$$

where, f'_c is the concrete compressive strength, a the distance from the point of maximum moment to point of zero moment, d the distance from extreme compression fibre to the centroid of longitudinal tension reinforcement, P the axial load, A_g the gross cross sectional area of column, A_v the area of transverse steel (= $\rho_v bs$), ρ_v the transverse reinforcement ratio, b the width of the column, and s the spacing of transverse reinforcement.

The model uses a factor k, which is assessed broadly from experimental data and depends on member displacement ductility. For shear-critical members (with displacement ductility of 1), the scatter of experimental data from the considered value of k is almost ± 20% [57]. In contrast, the proposed method does not use such an adjustment factor, but still provides a strength estimate in the same ball park of Method 2. Method 2 and the proposed method have similar normalized means (of 0.90 and 0.91 respectively), when all specimen are considered (Table 1). But, Method 2 estimates the shear strength of shear-critical specimens better with a slightly higher average (0.92) and smaller standard deviation (0.067), as against the proposed method which gives average of 0.89 and standard deviation of 0.078. Thus, while the NZ Guidelines provide simple expressions to estimate lateral shear strength of rectangular RC columns, the proposed method provides additional physically intuitive insight into the shear resistance mechanism without adjusting the model empirically.

Table 2: Details of experimental results and comparison of theoretical results.

S. No	Ref. No	Label	Loading Type	$B \times H$ mm x mm	f_c MPa	f_{yl} MPa	f_{yt} MPa	ρ_l %	ρ_t %	$\frac{M}{VH}$	Axial Load Ratio	V_{exp} kN	V_{prop} kN	Failure Mode		V_{theo}/V_{exp}				
														Exp.	Prop.	a	b	c	d	e
(1)	(2)	(3)	(4)	(5)	(6)	(7)	(8)	(9)	(10)	(11)	(12)	(13)	(14)	(15)	(16)	(17)	(18)	(19)	(20)	(21)
1	[39]	3	2C	400 × 400	23.6	427	320	1.51	1.76	4.39	0.27	192	179	F	F	0.86	0.86	0.86	0.97	0.93
2		4	2C	400 × 400	25.0	427	280	1.51	1.39	4.41	0.16	169	166	F	F	0.91	0.91	0.91	0.95	0.98
3	[42]	1	2C	400 × 400	46.5	446	364	1.51	0.78	4.43	0.16	200	186	F	F	0.88	0.88	0.88	0.88	0.93
4		2	2C	400 × 400	44.0	446	360	1.51	1.10	4.31	0.30	279	251	F	F	0.91	0.91	0.91	0.97	0.90
5		3	2C	400 × 400	44.0	446	364	1.51	0.73	4.28	0.28	277	249	F	F	0.93	0.93	0.93	0.97	0.90
6		4	2C	400 × 400	40.0	446	255	1.51	0.52	4.31	0.29	265	232	F	F	0.90	0.90	0.90	0.93	0.88
7	[43]	7	2C	400 × 400	28.3	440	466	1.51	1.13	4.67	0.18	213	181	F	F	0.76	0.76	0.76	0.81	0.85
8		8	2C	400 × 400	40.1	440	466	1.51	1.44	5.15	0.33	269	241	F	F	0.78	0.78	0.78	0.88	0.90
9	[46]	5	2C	400 x 400	41.0	474	372	1.51	1.06	4.58	0.44	292	233	F	F	0.83	0.83	0.83	0.99	0.80
10	[47]	1	2C	400 × 400	25.6	474	333	1.57	1.46	4.34	0.16	167	159	F	F	0.93	0.93	0.93	0.99	0.95
11		5	2C	550 × 550	32.0	511	325	1.25	1.42	3.32	0.09	386	367	F	F	0.89	0.89	0.89	0.91	0.95
12		7	2C	550 × 550	32.1	511	325	1.25	1.16	3.31	0.25	588	480	F	F	0.81	0.81	0.81	0.87	0.82
13	[37]	2S1	2C	305 × 305	30.7	367	363	1.63	0.48	6.07	0.09	61	56	F	F	0.84	0.84	0.84	0.84	0.92
14		3S1	2C	305 × 305	29.2	367	363	1.63	0.80	6.04	0.10	57	55	F	F	0.90	0.90	0.90	0.90	0.96
15		4S1	2C	305 × 305	27.6	429	363	1.63	0.48	5.96	0.18	49	60	F	F	1.16	1.16	1.16	1.16	1.22
16		5S1	2C	305 × 305	29.4	429	392	1.63	0.80	6.16	0.18	74	73	F	F	0.93	0.93	0.93	0.93	0.99
17		6S1	2C	305 × 305	31.8	429	392	1.63	0.48	6.25	0.17	75	74	F	F	0.91	0.91	0.91	0.92	0.99
18		9	2C	305 × 305	33.3	363	392	1.63	0.80	6.14	0.18	79	79	F	F	0.97	0.97	0.97	0.98	1.00
19		10	2C	305 × 305	32.4	363	392	1.63	0.48	6.35	0.27	78	79	F	F	0.95	0.95	0.95	0.96	1.01
20		12	2C	305 × 305	31.8	363	373	1.63	0.48	6.60	0.27	78	78	F	F	0.91	0.91	0.91	0.92	1.00
21	[38]	Gill1	2C	550 × 550	23.1	375	297	1.79	1.11	2.32	0.24	657	556	F	F	0.85	0.85	0.85	0.89	0.85
22		Gill2	2C	550 × 550	41.4	375	316	1.79	1.70	2.27	0.28	764	766	F	F	0.99	0.99	0.99	1.02	1.00
23		Gill3	2C	550 × 550	21.4	375	297	1.79	1.18	2.31	0.44	642	519	F	F	0.90	0.90	0.90	0.99	0.81
24		Gill4	2C	550 × 550	23.5	375	294	1.79	2.06	2.36	0.68	697	541	F	F	0.81	0.81	0.81	1.02	0.78
25	[50]	BG1	C	350 × 350	34.0	456	570	1.95	1.16	5.41	0.38	169	140	F	F	0.87	0.87	0.87	0.95	0.83
26		BG2	C	350 × 350	34.0	456	570	1.95	1.16	5.32	0.35	164	143	F	F	0.90	0.90	0.90	1.02	0.87
27		BG3	C	350 × 350	34.0	456	570	1.95	0.76	5.21	0.16	148	131	F	F	0.88	0.88	0.88	0.92	0.89
28		BG4	C	350 × 350	34.0	456	570	2.93	0.77	5.60	0.36	171	163	F	F	0.94	0.94	0.94	1.09	0.95
29		BG5	C	350 × 350	34.0	456	570	2.93	1.54	5.55	0.33	173	168	F	F	0.94	0.94	0.94	1.11	0.97
30		BG6	C	350 × 350	34.0	478	570	2.29	1.48	5.53	0.38	188	159	F	F	0.90	0.90	0.90	0.98	0.85
31		BG7	C	350 × 350	34.0	456	580	2.93	0.76	5.52	0.35	178	165	F	F	0.93	0.93	0.93	1.08	0.93
32		BG8	C	350 × 350	34.0	456	580	2.93	0.76	5.19	0.18	180	162	F	F	0.93	0.93	0.93	0.98	0.90
33		BG9	C	350 × 350	34.0	428	580	3.28	0.77	5.58	0.36	185	162	F	F	0.89	0.89	0.89	1.04	0.88
34		BG10	C	350 × 350	34.0	428	570	3.28	1.57	5.55	0.34	177	161	F	F	0.93	0.93	0.93	1.10	0.91
35	[52]	C1-1	C	400 × 400	24.9	497	460	2.13	0.95	3.66	0.08	250	187	F	F	0.85	0.85	0.85	0.90	0.75
36		C1-2	C	400 × 400	26.7	497	460	2.13	0.95	3.71	0.11	243	198	F	F	0.86	0.86	0.86	0.92	0.81
37		C1-3	C	400 × 400	26.1	497	460	2.13	0.02	4.10	0.15	243	208	F	F	0.79	0.79	0.79	0.84	0.86
38		C2-1	C	400 × 400	25.3	497	460	2.13	0.01	4.10	0.08	241	188	F	F	0.87	0.87	0.87	0.92	0.78

S. No	Ref. No	Label	Loading Type	$B \times H$ mm x mm	f_c MPa	f_{yl} MPa	f_{yt} MPa	ρ_l %	ρ_t %	$\frac{M}{VH}$	Axial Load Ratio	V_{exp} kN	V_{prop} kN	Failure Mode		V_{theo}/V_{exp}				
														Exp.	Prop.	a	b	c	d	e
(1)	(2)	(3)	(4)	(5)	(6)	(7)	(8)	(9)	(10)	(11)	(12)	(13)	(14)	(15)	(16)	(17)	(18)	(19)	(20)	(21)
39		C2-2	C	400 × 400	27.1	497	460	2.13	0.01	4.10	0.11	250	199	F	F	0.88	0.88	0.88	0.93	0.80
40		C2-3	C	400 × 400	26.8	497	460	2.13	0.01	4.10	0.15	271	209	F	F	0.79	0.79	0.79	0.83	0.77
41		C3-1	C	400 × 400	26.4	497	460	2.13	0.01	4.10	0.07	228	188	F	F	0.93	0.93	0.93	0.97	0.82
42		C3-2	C	400 × 400	27.5	497	460	2.13	0.01	4.10	0.11	248	199	F	F	0.89	0.89	0.89	0.94	0.80
43		C3-3	C	400 × 400	26.9	497	460	2.13	0.01	4.10	0.15	286	209	F	F	0.81	0.81	0.81	0.86	0.73
44	[40]	HPRC10-63	DC	200 × 200	21.6	371	344	1.27	1.22	1.55	0.13	87	87	F	F	0.97	0.97	0.97	0.91	1.00
45		HPRC19-32	DC	200 × 200	21.0	371	344	1.27	2.14	1.53	0.26	111	103	F	F	0.97	0.97	0.97	0.94	0.93
46	[47]	85PDC-1	DC	300 × 250	24.8	374	352	1.35	0.54	3.11	0.09	85	72	F	F	0.79	0.79	0.79	0.77	0.85
47		85PDC-2	DC	300 × 250	27.9	374	506	1.35	0.54	3.15	0.09	75	72	F	F	0.89	0.89	0.89	0.88	0.96
48		85PDC-3	DC	300 × 250	27.9	374	506	1.35	0.54	3.15	0.09	75	72	F	F	0.89	0.89	0.89	0.88	0.96
49		85STC-1	DC	300 × 250	27.9	374	506	1.35	0.54	3.16	0.08	76	75	F	F	0.88	0.88	0.88	0.86	0.99
50		85STC-2	DC	300 × 250	27.9	374	506	1.35	0.54	3.10	0.08	80	75	F	F	0.85	0.85	0.85	0.83	0.94
51		85STC-3	DC	300 × 250	27.9	374	506	1.35	0.54	3.16	0.08	76	75	F	F	0.88	0.88	0.88	0.86	0.99
52	[48]	H-2-1/5	DC	200 × 200	23.1	362	364	2.65	0.85	2.09	0.20	108	93	F	F	0.89	0.89	0.89	0.85	0.86
53		HT-2-1/5	DC	200 × 200	20.2	362	364	2.65	0.57	2.09	0.20	108	88	F	F	0.85	0.85	0.85	0.78	0.81
54		H-2-1/3	DC	200 × 200	23.1	362	364	2.65	1.06	2.11	0.33	121	98	F	F	0.83	0.83	0.83	0.85	0.81
55		HT-2-1/3	DC	200 × 200	20.2	362	364	2.65	0.71	2.13	0.33	118	90	F	F	0.79	0.79	0.79	0.79	0.76
56		H-1-1/8	DC	200 × 200	24.6	333	354	2.65	2.12	1.03	0.13	173	170	S	S	1.02	1.02	1.02	0.87	0.98
57		HT-1-1/8	DC	200 × 200	29.5	333	354	2.65	1.41	1.04	0.13	199	190	F	F	0.93	0.92	0.93	0.78	0.95
58		H-1-1/3	DC	200 × 200	22.9	333	354	2.65	2.12	1.05	0.33	187	195	S	F	1.03	1.03	1.03	0.88	1.04
59		HT-1-1/3	DC	200 × 200	22.5	333	354	2.65	1.41	1.05	0.33	184	185	F	F	1.04	1.04	1.04	0.84	1.01
60	[45]	U3	C	350 × 350	34.8	430	470	3.21	0.89	3.04	0.10	267	273	F	F	1.05	1.05	1.05	1.05	1.02
61		U4	C	350 × 350	32.0	438	470	3.21	1.33	3.17	0.10	324	269	F	F	0.82	0.82	0.82	0.83	0.83
62		U6	C	350 × 350	37.3	437	425	3.21	1.26	3.16	0.10	341	316	F	F	0.81	0.81	0.81	0.81	0.93
63		U7	C	350 × 350	39.0	437	425	3.21	1.26	3.16	0.10	340	316	F	F	0.81	0.81	0.81	0.82	0.93
64	[52]	15	DC	300 × 300	26.1	447	398	2.36	1.11	1.68	0.23	328	300	F	F	0.88	0.88	0.88	0.85	0.91
65	[54]	8	DC	300 × 300	30.7	402	392	1.05	0.18	2.20	0.20	174	154	F	S	0.91	0.91	0.85	0.84	0.89
66		6	DC	300 × 300	30.7	402	392	1.77	0.26	2.16	0.20	219	187	FS	FS	0.94	0.94	0.83	0.83	0.85
67		7	DC	300 × 300	30.7	402	392	1.77	0.18	2.18	0.20	213	171	FS	FS	0.99	0.95	0.78	0.85	0.81
68	[41]	CUS	DC	230 × 410	34.9	441	414	3.01	0.32	1.13	0.14	324	268	S	S	1.33	0.88	1.09	1.12	0.83
69		2CUS	DC	230 × 410	42.0	441	414	3.01	0.32	1.14	0.27	412	423	S	S	1.39	0.86	1.09	1.03	1.03
70		CUW	DC	410 × 230	34.9	441	414	3.01	0.64	2.03	0.14	265	229	S	S	1.15	1.08	1.04	0.99	0.86
71	[36]	25.033	2C	152 × 305	33.6	496	345	2.45	0.27	3.00	0.07	84	66	S	S	0.93	0.93	0.93	0.93	0.79
72		40.033	2C	152 × 305	33.6	496	345	2.45	0.27	3.02	0.11	89	88	S	S	0.92	0.92	0.92	0.91	0.99
73		40.033a	2C	152 × 305	34.7	496	345	2.45	0.27	3.04	0.11	95	91	S	S	0.93	0.93	0.93	0.92	0.96
74		40.048	2C	152 × 305	26.1	496	345	2.45	0.38	3.03	0.15	98	90	S	S	0.88	0.88	0.88	0.87	0.92
75		40.067	2C	152 × 305	33.4	496	345	2.45	0.53	3.17	0.11	89	96	S	S	0.94	0.94	0.94	0.94	1.08
76		40.092	2C	152 × 305	33.5	496	345	2.45	0.76	3.15	0.11	111	118	S	S	0.76	0.76	0.76	0.76	1.06
77		40.147	2C	152 × 305	33.5	496	345	2.45	1.21	3.14	0.11	109	94	--	FS	0.78	0.78	0.78	0.78	0.86

S. No	Ref. No	Label	Loading Type	$B \times H$ mm x mm	f_c MPa	f_{yl} MPa	f_{yt} MPa	ρ_l %	ρ_t %	$\frac{M}{VH}$	Axial Load Ratio	V_{exp} kN	V_{prop} kN	Failure Mode		V_{theo}/V_{exp}				
														Exp.	Prop.	a	b	c	d	e
(1)	(2)	(3)	(4)	(5)	(6)	(7)	(8)	(9)	(10)	(11)	(12)	(13)	(14)	(15)	(16)	(17)	(18)	(19)	(20)	(21)
78	[51]	3CLH18	DC	457 × 457	26.9	331	399	3.04	0.10	3.28	0.08	277	242	S	S	1.08	0.83	0.98	0.91	0.87
79		2CLH18	DC	457 × 457	33.1	331	399	1.94	0.10	3.35	0.07	241	216	S	S	0.91	0.91	0.91	0.83	0.90
80		3SLH18	DC	457 × 457	26.9	331	399	3.04	0.10	3.26	0.08	270	242	S	S	1.11	0.86	1.01	0.93	0.90
81		2SLH18	DC	457 × 457	33.1	331	399	1.94	0.10	3.30	0.07	229	204	S	S	0.97	0.97	0.97	0.88	0.89
82		2CMH18	DC	457 × 457	25.5	331	399	1.94	0.10	3.37	0.27	306	241	S	FS	0.91	0.91	0.91	0.87	0.79
83		3CMH18	DC	457 × 457	27.6	331	399	3.04	0.10	3.36	0.27	328	295	S	S	1.08	0.92	0.97	0.95	0.90
84		3CMD12	DC	457 × 457	27.6	331	399	3.04	0.25	3.37	0.22	355	312	S	S	0.99	0.99	0.99	0.97	0.88
85		CSMD12	DC	457 × 457	25.5	331	399	3.04	0.25	3.43	0.24	367	301	S	S	0.92	0.92	0.92	0.91	0.82
86	[22]	SC-2.4-0.2	DC	350 × 350	22.6	409	393	2.05	0.21	2.58	0.20	219	200	S	S	1.03	0.95	0.95	0.90	0.91
87		SC-2.4-0.3	DC	350 × 350	49.3	409	393	3.21	0.21	2.80	0.30	357	382	S	S	1.14	0.94	0.98	1.06	1.07
88		SC-2.4-0.5	DC	350 × 350	24.2	409	393	2.05	0.21	2.88	0.50	238	207	S	FS	0.96	0.96	0.96	0.96	0.87
89		SC-1.7-0.05	DC	350 × 350	29.8	409	393	2.05	0.21	1.74	0.05	276	215	S	S	1.03	0.80	0.81	0.79	0.78
90		SC-1.7-0.2	DC	350 × 350	27.5	409	393	2.05	0.21	1.82	0.20	294	272	S	S	1.19	0.96	0.93	0.96	0.93
91		SC-1.7-0.35	DC	350 × 350	25.5	409	393	2.05	0.21	1.86	0.35	336	282	S	S	1.06	0.95	0.91	0.87	0.84
92		SC-1.7-0.5	DC	350 × 350	26.4	409	393	2.05	0.21	1.91	0.50	376	300	S	FS	0.96	0.96	0.93	0.79	0.80
93		RC-1.7-0.05	DC	250 × 490	32.5	409	393	2.05	0.21	1.79	0.05	283	229	S	S	1.01	0.90	0.88	0.88	0.81
94		RC-1.7-0.2	DC	250 × 490	24.5	409	393	2.05	0.21	1.84	0.20	306	261	S	S	1.00	0.95	0.91	0.90	0.85
95		RC-1.7-0.35	DC	250 × 490	27.1	409	393	2.05	0.21	1.91	0.35	346	296	S	S	0.97	0.97	0.93	0.93	0.86
96		RC-1.7-0.5	DC	250 × 490	26.8	409	393	2.05	0.21	1.98	0.50	355	286	S	S	0.93	0.93	0.93	0.86	0.81
97	[53]	1	DC	300 × 300	27.7	447	398	1.77	0.55	1.03	0.22	341	316	S	S	1.16	0.85	0.96	0.88	0.93
98		11	DC	300 × 300	28.2	447	398	2.36	0.18	1.56	0.21	243	206	S	S	1.15	0.87	0.88	0.97	0.85
99		12	DC	300 × 300	28.2	447	398	2.36	0.18	1.57	0.21	250	206	S	S	1.11	0.84	0.85	0.94	0.82
100		13	DC	300 × 300	26.1	447	398	2.36	0.55	1.58	0.23	266	273	S	S	1.15	1.08	1.04	1.03	1.03
101		14	DC	300 × 300	26.1	447	398	2.36	0.55	1.60	0.23	296	273	S	S	1.02	0.96	0.93	0.92	0.92
102		16	DC	300 × 300	26.1	447	398	1.77	0.55	1.04	0.23	341	306	S	S	1.12	0.83	0.95	0.84	0.90
103	[54]	1	DC	300 × 300	30.7	402	392	2.68	0.26	2.09	0.20	234	208	S	S	1.14	0.97	0.85	0.93	0.89
104		2	DC	300 × 300	30.7	402	392	2.68	0.18	2.06	0.20	230	190	S	S	1.10	0.92	0.79	0.92	0.83
105		3	DC	300 × 300	30.7	402	392	2.68	0.13	2.10	0.20	230	197	S	S	1.03	0.86	0.76	0.88	0.86
106		4	DC	300 × 300	30.7	402	392	2.68	0.26	2.13	0.30	261	234	S	S	1.03	0.96	0.82	0.92	0.90
107		5	DC	300 × 300	30.7	402	392	2.68	0.26	2.18	0.35	275	233	S	S	0.96	0.93	0.81	0.88	0.85

a Method 1 [2] - Priestley *et al.*, (1994) c Method 3 [23] - Pan, and Li, (2012) e Proposed Method F Flexure

b Method 2 [22] - Sezen, (2002) d Method 4 [24] - Rossi (2013) S Shear FS Combined Flexure-Shear

Symbol	*Description*	*Symbol*	*Description*	*Symbol*	*Description*
C	Cantilever member	V_{prop}	Failure load using proposed model	ρ_l	Longitudinal reinforcement ratio
2C	Double ended cantilever member	V_{theo}	Theoretical estimates of lateral load capacity	ρ_t	Transverse reinforcement ratio
DC	Member in double bending	f_c	Compressive strength of concrete	M	Bending moment of a cross section
B	Width of the member cross-section	f_{yl}	Yield strength of longitudinal rebar	V_{exp}	Estimated failure load from experiments
H	Depth of the member cross-section	f_{yt}	Yield strength of transverse reinforcement		

CONCLUSION

A simple analytical procedure is presented for estimating the failure load and for capturing the failure mode and failure location in RC members with rectangular cross-section. Comparison of estimates from the Proposed Method with experimental results available in literature suggests that the proposed method provides results with reliable accuracy for a large range of (L/H) ratio. The method helps in identifying the possible mode of damage for assessment of existing RC members. In addition, the proposed *V-M* interaction diagram explains in a simple way the shear resistance mechanism of RC members under combined action of *P-V-M*. In the Proposed Method, the following effects are not considered: (a) strain compatibility, (b) strain rate including that of reversed cyclic loading, and (c) deficiencies in detailing of reinforcing bars and bond strength.

REFERENCES

1 Lee DH and Elnashai AS (2001). "Seismic analysis of RC bridge columns with flexure-shear interaction". *Journal of Structural Engineering ASCE*, **127**(5): 546-553. https:/doi.org/10.1061/(ASCE)0733-9445(2001)127:5(546)

2 Priestley MJN, Verma R and Xiao Y (1994). "Seismic shear strength of reinforced concrete columns". *Journal of Structural Engineering ASCE*, **120**(8): 2310-2329. https://doi.org/10.1061/(ASCE)0733-9445(1994)120:8(2310)

3 Collins MP and Mitchell D (1991). "*Prestressed Concrete Structures*". Englewood Cliffs, Prentice Hall, NJ, ISBN: 978-0-136916-35-2, 766 pp.

4 Tegos IA and Penelis G (1988). "Seismic resistance of short columns and coupling beams reinforced with inclined bars". *ACI Structural Journal*, **85**(1): 82-88.

5 Moretti ML and Tassios TP (2006). "Behaviour and ductility of reinforced concrete short columns using global truss model". *ACI Structural Journal*, **103**(3): 319–327.

6 Moretti ML and Tassios TP (2013). "Design in shear of reinforced concrete short columns". *Earthquakes and Structures*, **4**(3): 265–283. https://doi.org/10.12989/eas.2013.4.3.265

7 Park H and Eom T (2007). "Truss model for nonlinear analysis of RC members subject to cycling loading". *ASCE Journal of Structural Engineering*, **133:** 1351-1363. https://doi.org/10.1061/(ASCE)0733-9445(2007)133:10(1351)

8 Tureyen AK and Frosch RJ (2003). "Concrete shear strength: Another perspective". *ACI Structural Journal*, **100**(5): 609-615. https://doi.org/10.14359/12802

9 Park HG, Choi KK and Wight JK (2006). "Strain-based shear strength model for slender beams without web reinforcement". *ACI Structural Journal*, **103**(6): 783-793. https://doi.org/10.14359/18228

10 Park HG, Yu EJ and Choi KK (2012). "Shear-strength degradation model for RC columns subjected to cyclic loading". *Engineering Structures*, **34**: 187-197. https://doi.org/10.1016/j.engstruct.2011.08.041

11 Mari A, Bairan J, Cladera C, Oller E and Ribas C (2014). "Shear-flexural strength mechanical model for the design and assessment of reinforced concrete beams". *Structure and Infrastructure Engineering: Maintenance, Life-Cycle Design and Performance*, **8**(4): 337-353. https://doi.org/10.1080/15732479.2014.964735

12 Cladera A, Marí A, Bairán J, Oller E and Ribas C (2015). "Predicting the shear-flexural strength of slender reinforced concrete T and I shaped beams". *Engineering Structures*, **101**: 386-398. https://doi.org/10.1016/j.engstruct.2015.07.025

13 ACI-ASCE Committee 426 (1973). "The shear strength of reinforced concrete members". *ACI Journal Proceedings*, **70**: 1091–1187.

14 Collins MP, Mitchell D, Adebar P and Vecchio FJ (1996). "A general shear design method". *ACI Structural Journal*, **93**(1): 36-45. https://doi.org/10.14359/9838

15 Kupfer H (1964). "Generalization of Morsch's truss analogy using principle of minimum strain energy". *CEB Bulletin d'Information*, No.40, Comite Ero-International du Beton, No.40: 44-57.

16 Lampert P and Thurlimann B (1971). "*Ultimate Strength and Design of Reinforced Concrete Beams in Torsion and Bending*". Publication No. IABSE 31-I, IABSE, Zurich, 107-131. https://doi.org/10.1007/978-3-0348-5954-7_1

17 CEB-FIP. (1978). "*Model Code for Concrete Structures".* CEB-FIB International Recommandations. 3rd ed, Comite Euro-International Du Beton, Paris, 471 pp.

18 Ramirez JA and Breen JE (1991). "Evaluation of a modified truss-model approach for beams in shear". *ACI Structural Journal*, **88**(5): 562-571. https://doi.org/10.14359/3145

19 Vecchio FJ and Collins MP (1986). "The modified compression field theory for reinforced concrete elements subjected to shear". *ACI Structural Journal*, **83**(2): 219-231. https://doi.org/10.14359/10416

20 Vecchio FJ and Collins MP (1988). "Predicting the response of reinforced concrete beams subjected to shear using the modified compression field theory". *ACI Structural Journal*, **85**(3): 258-268. https://doi.org/10.14359/2515

21 Hsu TTC (1988). "Softened truss model theory for shear and torsion". *ACI Structural Journal*, **85**(6): 624–635. https://doi.org/10.14359/2740

22 Sezen H (2002). "*Seismic Behaviour and Modelling of Reinforced Concrete Building Columns*". Ph.D. Dissertation, Berkeley, Department of Civil and Environmental Engineering, University of California, USA, 336 pp.

23 Pan Z and Li B (2012). "Truss–Arch model for shear strength of shear-critical reinforced concrete columns". *ASCE Journal of Structural Engineering*, **139**(4): 548-560. https://doi.org/10.1061/(ASCE)ST.1943-541X.0000677

24 Rossi PP (2013). "Evaluation of the ultimate strength of RC rectangular columns subjected to axial force, bending moment and shear force". *Engineering Structures*, **57**: 339-355. https://doi.org/10.1016/J.ENGSTRUCT.2013.09.006

25 Mergos PE and Kappos AJ (2008). "A distributed shear and flexural flexibility model with shear–flexure interaction for RC members subjected to seismic loading". *Earthquake Engineering and Structural Dynamics*, **37**: 1349–1370. https://doi.org/10.1002/EQE.812

26 Mergos PE and Kappos AJ (2010). "Seismic damage analysis including inelastic shear–flexure interaction". *Bulletin of Earthquake Engineering*, **8**: 27–46. https://doi.org/10.1007/S10518-009-9161-2

27 Mergos PE and Kappos AJ (2012). "A gradual spread inelasticity model for RC beam-columns, accounting for flexure, shear and anchorage slip". *Engineering Structures*, **44:** 94–106. https://doi.org/10.1016/J.ENGSTRUCT.2012.05.035

28 Kolozvari K, Orakcal K and Wallace JW (2015a). "Shear-flexure interaction modelling of reinforced concrete structural walls and columns under reversed cyclic loading", Pacific Earthquake Engineering Research Center, University of California, Berkeley, PEER Report No. 2015/12.

29 Petrangeli M, Pinto PE and Ciampi V (1999). "Fiber element for cyclic bending and shear of RC structures, Part I: Theory". *ASCE Journal of Engineering Mechanics*, **125**(9): 994-1010. https://doi.org/10.1061/(ASCE)0733-9399(1999)125:9(994)

30 Marini A and Spacone E (2006). "Analysis of reinforced concrete elements including shear effects". *ACI Structural Journal*, **103**(5): 645–655. https://doi.org/10.14359/16916

31 Bresler B and Pister KS (1958). "Strength of concrete under combined stresses". *ACI Structural Journal*, **55**(9): 321-345.

32 IS 456: 2000 (2000). "*Indian Standard Code of Practise for Plain and Reinforced Concrete*". Bureau of Indian Standards, New Delhi, India, 107 pp.

33 Mander JB, Priestly MJN and Park R (1988). "Theoretical Stress-strain model for confined concrete". *ASCE Journal of Structural Engineering*, **114**(8): 1804-1826. https://doi.org/10.1061/(ASCE)0733-9445(1988)114:8(1804)

34 FIB (2003). "*Displacement-based Seismic Design of Reinforced Concrete Buildings*". Fib Bulletin 25, State-of-Art Report Prepared by Task Group 7.2, Lausanne, 196 pp. https://doi.org/10.35789/FIB.BULL.0025

35 Chen WF (2007). "*Plasticity in Reinforced Concrete*". J Ross Publishing, New York, USA, ISBN: 978-1-932159-74-5, 474 pp.

36 Wight JK and Sozen MA (1973). "*Shear strength decay in reinforced concrete columns subjected to large deflection reversals*". Structural research series no. 403, Civil Engineering Studies, University of Illinois, Urbana–Champaign, IL, USA, 285 pp.

37 Atalay MB and Penzien J (1975). "*The seismic behavior of critical regions of reinforced concrete components as influenced by moment, shear and axial force*". Report No. EERC 75-19, University of California, Berkeley, 226 pp.

38 Gill WD, Park R and Priestley MJN (1979). "*Ductility of rectangular reinforced concrete columns with axial load*." Report 79-1, Department of Civil Engineering, University of Canterbury, Christchurch, New Zealand, 136 pp.

39 Ang BG (1981). "*Ductility of reinforced concrete bridge piers under seismic loading*". Report 81-3, Department of Civil Engineering, University of Canterbury, Christchurch, New Zealand, 113 pp.

40 Nagasaka T (1982). "Effectiveness of steel fiber as web reinforcement in reinforced concrete column". *Trans Japan Concrete Institute*, **4**: 493–500.

41 Umehara H and Jirsa JO (1982). "*Shear strength and deterioration of short reinforced concrete columns under cyclic deformations*". PMFSEL Report No. 82-3, Department of Civil Engineering, University of Texas at Austin, Austin, Texas, 256 pp.

42 Soesianawati MT, Park R and Priestley MJN (1986). "*Limited ductility design of reinforced concrete columns*". Report 86-10, Department of Civil Engineering, University of Canterbury, Christchurch, New Zealand, 208 pp.

43 Zahn FA, Park R and Priestley MJN (1986). "*Design of reinforced bridge columns for strength and ductility*". Report 86-7, Department of Civil Engineering, University of Canterbury, Christchurch, New Zealand, 330 pp.

44 Zhou X, Satoh T, Jiang W, Ono A and Shimizu Y (1985). "Behavior of reinforced concrete short column under high axial load". *Trans Japan Concrete Institute*, **9**: 541–548.

45 Saatcioglu M and Ozcebe G (1989). "Response of reinforced concrete columns to simulated seismic loading". *ACI Structural Journal*, **86**(1): 3-12. https://doi.org/10.14359/2607

46 Watson S and Park R (1989). "*Design of reinforced concrete frames of limited ductility*". Report 89-4, Department of Civil Engineering, University of Canterbury, Christchurch, New Zealand, 232 pp.

47 Tanaka H and Park R (1990). "*Effect of lateral confining reinforcement on the ductile behavior of reinforced concrete columns*". Report 90-2, Department of Civil Engineering, University of Canterbury, Christchurch, New Zealand, 458 pp.

48 Esaki F (1996). "Reinforcing effect of steel plate hoops on ductility of R/C square column". *Proceedings of the 11th World Conference on Earthquake Engineering*, June 23-29 1996, Paper No. 199, 406 pp.

49 Taylor AW, Kuo C, Wellenius K and Chung D (1997). "*A summary of cyclic lateral load tests on rectangular reinforced concrete columns*". National Institute of Standards and Technology Report NISTIR 5984, 95 pp. https://doi.org/10.6028/NIST.IR.5984

50 Saatcioglu M and Grira M (1999). "Confinement of reinforced concrete columns with welded reinforcement grids". *ACI Structural Journal*, **96**(1): 29-39. https://doi.org/10.14359/593

51 Lynn A (1999). "*Seismic evaluation of existing reinforced concrete building columns*". Ph.D. Thesis, University of California at Berkeley, Berkley (CA), 284 pp.

52 Mo YL and Wang SJ (2000). "Seismic behavior of RC columns with various tie configurations," *ASCE Journal of Structural Engineering*, **126**(10): 1122–1130. https://doi.org/10.1061/(ASCE)0733-9445(2000)126:10(1122)

53 Ousalem H, Kabeyasawa T, Tasai A and Iwamoto J (2003). "Effect of hysteretic reversals on lateral and axial capacities of reinforced concrete columns". *Proceedings of the Annual Conference of Japan Concrete Institute*, Kyoto, Japan, **25**(2): 367–372.

54 Yoshimura M and Nakamura T (2003). "Axial collapse of reinforced concrete short columns". *Proceedings of the Fourth US–Japan Workshop on Performance Based Earthquake Engineering Methodology for Reinforced Concrete Building Structures*, Toba, Japan, 187–198.

55 Bazant ZP and Kwon YW (1994). "Failure of slender and stocky reinforced concrete columns: Tests of size effect". *Materials and Structures*, **27**: 79–90. https://doi.org/10.1007/BF02472825

56 Ohtaki T (2000). "An experimental study on scale effects in shear failure of reinforced concrete columns". *In Proceedings of 12th World Conference on Earthquake Engineering 2000*, 2186/6/A, 30 January-4 February, Paper No. 2186.

57 Sezen H and Moehle JP (2004). "Shear strength model for lightly reinforced concrete columns". *ASCE Journal of Structural Engineering*, **130**(11): 1692-1703. https://doi.org/10.1061/(ASCE)0733-9445(2004)130:11(1692)